

Supporting information for:
From the metal to the channel: a study of the
carrier injection through metal / MoS₂
interface.

Goutham Arutchelvan^{=,*†‡} César J. Lockhart de la Rosa^{=,†‡} Phillipe Matagne,[†]
Surajit Sutar,[†] Iuliana Radu,[†] Cedric Huyghebaert,[†] Stefan De Gendt,^{†,¶} and Marc
Heyns^{†,‡}

†imec, Kapeldreef 75, B-3001 Leuven, Belgium

*‡Department of Metallurgy and Materials Engineering, KU Leuven, Kasteelpark Arenberg
44, B-3001 Leuven, Belgium*

¶Department of Chemistry, K. U. Leuven, Celestijnenlaan 200F, B-3001 Leuven, Belgium

E-mail: goutham.arutchelvan@imec.be

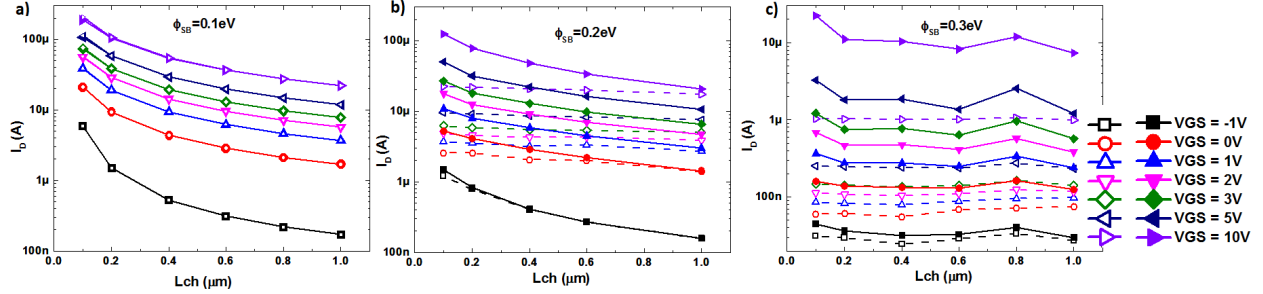


Figure S1: Total current (I_D) with only thermionic emission over SB (empty symbols) and both thermionic+tunneling through the SB (solid symbols) for different L_{CH} and ϕ_{SB} of (a) 0.1eV , (b) 0.2eV , (c) 0.3eV . Clearly, for the case of moderate ϕ_{SB} (b,c), carrier injection by tunneling through the Metal / MoS₂ increases as the V_{GS} increases. This can be explained by the thinning down of the SB as more carriers are accumulated in the MoS₂ film with increase in V_{GS} . Also, for a given V_{GS} , the tunneling current becomes significant with decrease in the L_{CH} .

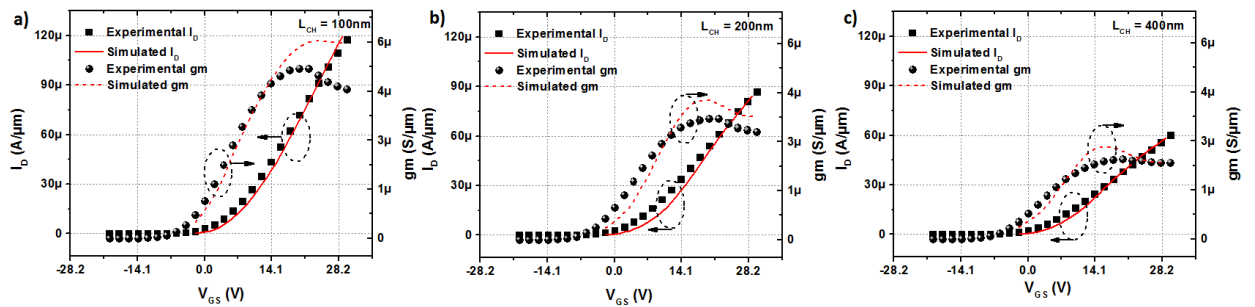


Figure S2: Transfer characteristics and transconductance for the simulated and experimental measurements of the TLM set A (a-c). The agreement between the transfer characteristics of experimental and simulated devices corroborates the validity of the model across different thicknesses.

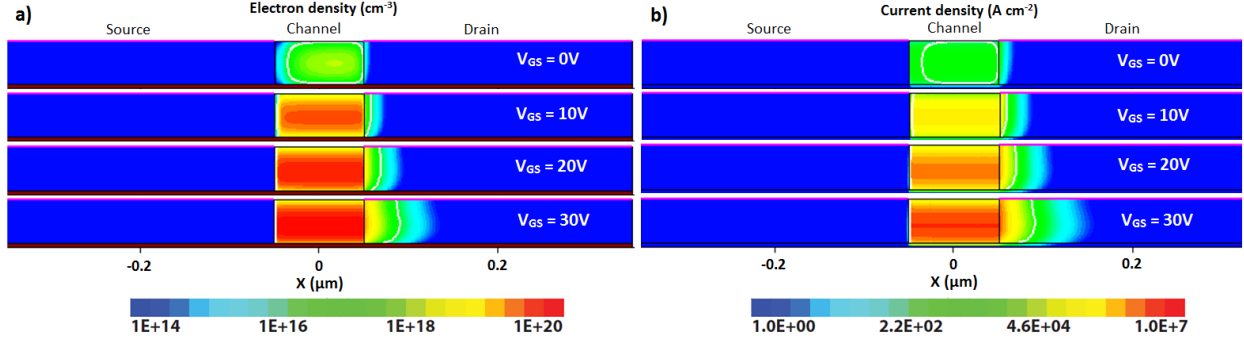


Figure S3: Surface plot of the electron density (a) and the current density (b) of the simulated device with $t_{\text{SC}} = 1.4 \text{ nm}$ and $L_{\text{CH}} = 100 \text{ nm}$ for different V_{GS} . The region under the source contact remains depleted for all V_{GS} and the lateral trajectory is the only relevant trajectory for the carrier injection from the source.

Effect of vertical mobility and out-of-plane tunneling mass

The effect of vertical mobility and out-of-plane tunneling mass on the two injection paths is briefly discussed here. A different vertical mobility value was used in the simulation to capture the anisotropy between the out-of-plane and in-plane electronic transport. It is convenient to define an anisotropy factor (r) as the ratio between $\mu_{\text{in-plane}}$ to μ_{\perp} . Accordingly, r equal to 10 and 100 was used in the simulated devices of $t_{\text{SC}} = 5.9 \text{ nm}$, shown in S4-(a,b) and S4-(c,d), respectively. Clearly, the lateral trajectory in case of low V_{GS} (S4-(a,c)) and lateral+vertical trajectories for high V_{GS} (S4-(b,d)) can be identified for the thick film. However, the injected carriers in the channel do not necessarily flow in the bottom layers but show significant conduction in the layers away from the $\text{MoS}_2/\text{SiO}_2$ interface. This effect is due to the increased resistance (lower $m\mu_{\perp}$) for the injected carriers to move in the perpendicular direction. As can be seen in S4-(e,f), the effect becomes less prominent for thin films where the tunneling distance from the metal to the accumulated region at $\text{MoS}_2/\text{SiO}_2$ is small. Consequently, the out-of-plane tunneling mass is an important parameter to consider for such cases. In S5, the effect of varying the out-of plane mass on the transfer characteristics of a simulated device with $t_{\text{SC}} = 5.9 \text{ nm}$ is shown. For $m=100$, nearly two order of magnitude drop in I_{D} can be seen. However, the two injection trajectories were clearly noticed in the current distribution plot of the same device and exhibited similar behavior with different

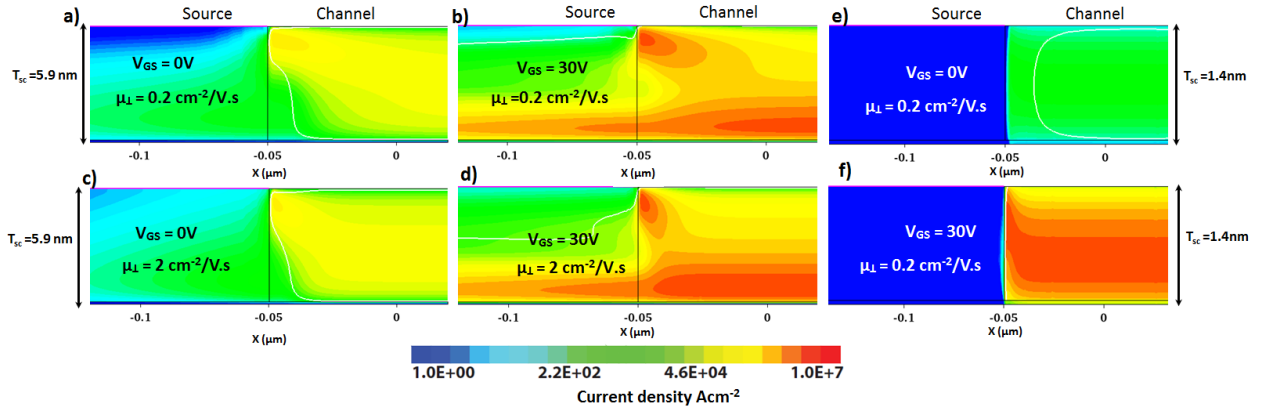


Figure S4: Magnified surface plot of the current density for the simulated device with $t_{SC} = 5.9 \text{ nm}$ (a-d) and $t_{SC} = 1.4 \text{ nm}$ (e,f) for different V_{GS} and a vertical mobility equal to $0.2 \text{ cm}^2 \text{ V}^{-1} \text{ s}^{-1}$ (a,b,e,f) and $2 \text{ cm}^2 \text{ V}^{-1} \text{ s}^{-1}$ (c,d). The two injection trajectories and their dependence on field and film thickness are similar to the previous discussions. However, the current flows not only in the bottom layers but also in the layers away from $\text{MoS}_2 / \text{SiO}_2$ interface due to the increased vertical resistance.

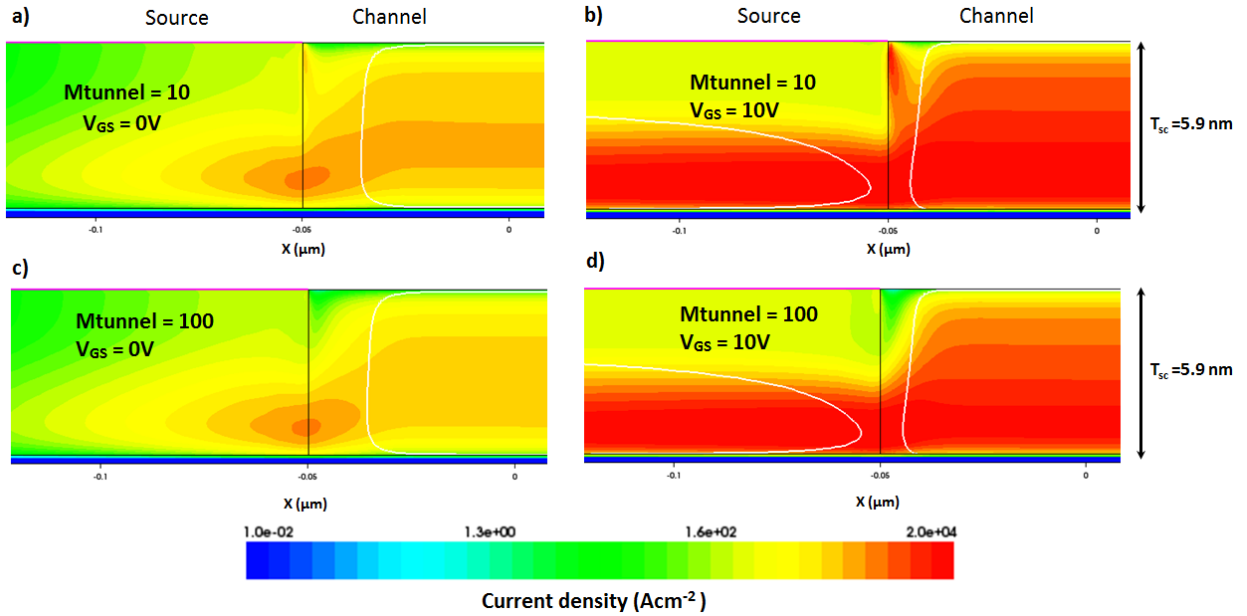


Figure S5: Magnified surface plot of the current density for the simulated device with $t_{SC} = 5.9 \text{ nm}$ with M_{tunnel} equal to (a,b) 10 and (c,d) 100 for two different V_{GS} . The current density is reduced compared to fig-4 due to the reduced transmission probability across the Schottky barrier. However, the lateral trajectory for low V_{GS} and both the trajectories (vertical+lateral) can be seen for high V_{GS} .

fields. Therefore, all the major conclusions previously stated regarding the trajectories and their dependence on V_{GS} and V_{DS} remain qualitatively the same.